
RECIPRO-CAM: GRADIENT-FREE RECIPROCAL CLASS ACTIVATION MAP

A PREPRINT

Seok-Yong Byun
Intel Corp.
Seoul, South Korea 06134
mark.byun@intel.com

Wonju Lee
Intel Corp.
Seoul, South Korea 06134
wonju.lee@intel.com

February 1, 2023

ABSTRACT

Convolutional neural network (CNN) becomes one of the most popular and prominent deep learning architectures for computer vision, but its black box feature hides the internal prediction process. For this reason, AI practitioners have shed light on explainable AI to provide the interpretability of the model behavior. In particular, class activation map (CAM) and Grad-CAM based methods have shown promise results, but they have architectural limitation or gradient computing burden. To resolve these, Score-CAM has been suggested as a gradient-free method, however, it requires more execution time compared to CAM or Grad-CAM based methods. Therefore, we propose a lightweight architecture and gradient free Reciprocal CAM (Recipro-CAM) by spatially masking the extracted feature maps to exploit the correlation between activation maps and network outputs. With the proposed method, we achieved the gains of 1.78 - 3.72% in the ResNet family compared to Score-CAM in Average Drop-Coherence-Complexity (ADCC) metric, excluding the VGG-16 (1.39% drop). In addition, Recipro-CAM exhibits a saliency map generation rate similar to Grad-CAM and approximately 148 times faster than Score-CAM. The source code of Recipro-CAM is available at our data analysis framework¹.

Keywords Explainable AI · Gradient-free CAM · Reciprocity

1 Introduction

Convolutional neural networks (CNNs) have achieved popularity in the AI community because of their cost-efficient and superior performance in the computer vision area. Even though CNN shows good performance in general uses, it sometimes doesn't work for edge cases or out-of-distribution inputs as expected manner. In this case, it is difficult to reveal the root cause because of its black box property. Explainable AI (XAI) has emerged to tackle this problem and give AI practitioners a explainable reason.

The first recognizable approach is the class activation map (CAM) (Zhou et al. [2016]) method that operates simply and provides reasonable results, but it has a serious weakness to become a general solution because the target model must consist of a global average/max pooling layer and a single fully connected (FC) layer as its classifier. In order to remove these restrictions, Grad-CAM has been proposed by Selvaraju et al. [2016], which uses gradient information of class confidence output with respect to the convolution layer's activation map and the activation map itself. This approach removed the architectural limitation of CAM but imposed a new gradient-related restriction, so this method requires a trainable network to work. Score-CAM (Wang et al. [2020a]) has been proposed as a novel mechanism for removing the gradient restriction from Grad-CAM operation by employing a black-box XAI approach. This provides the saliency map through inferring the perturbed images taken from the activation map of a given convolution layer and the original input. Therefore, its execution performance is dependent on input resolution, convolution channel dimensions and network capacity, and as a result, Score-CAM is approximately 127 \times slower than CAM or Grad-CAM methods.

¹https://github.com/openvinotoolkit/datumaro/blob/feats/recipro-cam/datumaro/components/algorithms/recipro_cam.py

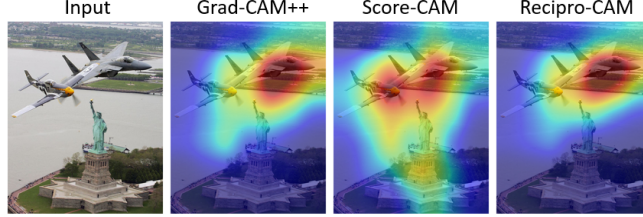


Figure 1: Resolution capability comparison of Grad-CAM++, Score-CAM, and Recipro-CAM. Predicted class is aircraft carrier but ground truth is warplane. Score-CAM cannot separate warplane from nearby object.

Recipro-CAM is inspired by CAM and RISE (Petsiuk et al. [2018]) methods in which the convolution layer’s activation map has a reciprocal relationship with the network’s output prediction directly and indirectly. With this insight, Recipro-CAM focuses on the reciprocal relationship between the convolution layer’s activation map and output prediction itself instead of using just the activation map and the last FC layer’s weight like CAM or using new input images generated from convolution activation map like Score-CAM as depicted at Figure 2. The detailed explanation will be provided at Section 3.

The contributions of this paper are as follows.

- We introduce a novel efficient gradient-free white-box XAI solution by leveraging the reciprocal relationship between convolution layer’s activation map and the network output. Recipro-CAM removes both architectural and gradient-computable constraints like Score-CAM, while achieving approximately $148\times$ faster execution performance than Score-CAM.
- We evaluate the accuracy of the Recipro-CAM for classification tasks using Average Drop, Average Increase, Deletion, Insertion, Coherency, Complexity, and Average DCC (ADCC) metrics with VGG-16, ResNet, and ResNeXt architectures and show state-of-the-art (SOTA) accuracy on ADCC metric except for VGG-16 architecture and show relatively good accuracy values for other metrics compared to other methods.

2 Related Work

The black box feature of DNN hides all internal processes and reactions from input to output, so AI practitioners are trying to reveal the internal process and neuron’s reaction mechanism according to input variation. Zeiler and Fergus [2014] and Springenberg et al. [2015] suggested a deconvolution approach to get each layer’s learned features and show important pixels in the input image in a class agnostic manner. From these studies, DNN’s layer-wise learning property started to understand, and this contributed to the development of DNN architecture. However, with this knowledge, researchers couldn’t understand the prediction result of DNN for specific input so researchers started to research methods that can explain the relationship between input data and DNN output.

The first approach is Class Activation Map (CAM) proposed by Zhou et al. [2016] as a class-specific saliency map solution. CAM generates a class activation map by multiplying a globally pooled channel-wise activation vector with a fully connected weight vector for the class. In short, the the saliency map S^c for class c is calculated by

$$S^c = \sum_k w_{k,c} \sum_{u,v} f_k(u,v) \quad (1)$$

where $w_{k,c}$ is the last FC layer’s weight between channel k and class c and $f_k(u,v)$ is the activation at (u,v) of channel k . With CAM method, AI practitioners can analyze not only their architecture’s capability but also the class-specific reaction of the network. However, CAM requires a global average or max pooling layer, and this restricts available architectures.

Grad-CAM (Selvaraju et al. [2016]), Grad-CAM++ (Chattopadhyay et al. [2018]), Axiom-based Grad-CAM (Fu et al. [2020]), and Smooth Grad-CAM++ (Omeiza et al. [2019]) proposed gradient-based saliency map generation methods to remove architectural limitations and generalized the CAM method. These methods mainly use the gradient information of class confidence output with respect to the given convolution layer’s activation map itself as

$$\mathcal{L}_{\text{Grad-GAM}}^c = \text{ReLU} \left(\sum_k \alpha_k^c A^k \right), \quad (2)$$

where

$$\alpha_k^c = \frac{1}{Z} \sum_i \sum_j \frac{\partial y^c}{\partial A_{ij}^k}. \quad (3)$$

Gradient-based approaches mitigated the architectural limitation of CAM and their explainability made them a popular solution for XAI, however, the methods require a trainable model for using gradient information. Therefore, these cannot be used in the deployed model such as ONNX (Bai et al. [2019]) or OpenVINO (Intel [2019]). Furthermore, the saturation and false confidence issues were found by (Wang et al. [2020a]) and to tackle this, they proposed Score-CAM and related Smooth Score-CAM (Wang et al. [2020b]). And Integrated Score-CAM (Naidu et al. [2020]) methods improved its performance.

Score-CAM extracts the channel-wise activation information from the convolution layers and upscales them to input image size, then generates a masked image with the channel-wise activation map. By using these masked images as new input images, Score-CAM calculates the channel-wise increase of confidence (CIC) for generating saliency map for the specified class. This improves the explainability of CNN results quantitatively and qualitatively without using gradient information, but this approach requires many inference operations depending on the number of channels of the convolution layer for the saliency map and it takes a longer time than CAM or Grad-CAM approaches.

Recently, Ablation-CAM has been proposed as a gradient-free approach Desai and Ramaswamy [2020]. This overcomes the saturation and gradient explosion problems of Grad-CAM by introducing the effective slope, which is calculated by the difference between the original prediction score and the prediction score from the ablated activation map. While the ablation drop Morcos et al. [2018] is helpful to describe how important an ablation unit is for a target class well, this requires to take much time because of iteration over each feature map to ablate.

Apart from these white-box approaches, there have been several studies on black-box approaches like Petsiuk et al. [2018], Kenny et al. [2021], Dabkowski and Gal [2017], Petsiuk et al. [2020]. They can generate a saliency map without any dependency on network architectural information or gradient computability, however, these methods take much longer time than white box methods and show relatively lower accuracy.

2.1 Evaluation Metrics

XAI solution itself also should be measured by exact unified metric, however, there was no standard unified metric except for Chattopadhyay et al. [2018], Petsiuk et al. [2018], Fu et al. [2020] suggested by each researcher until ADCC suggested by Poppi et al. [2021]. ADCC combines average drop, coherence, and complexity in a single metric taking their harmonic mean given by

$$\text{ADCC}(x) = 3 \left(\frac{1}{\text{Coherency}(x)} + \frac{1}{1 - \text{Complexity}(x)} + \frac{1}{1 - \text{AverageDrop}(x)} \right)^{-1}. \quad (4)$$

In this paper, we will evaluate our method's accuracy with the ADCC metric.

3 Recipro-CAM

The proposed Recipro-CAM is a gradient and architecture-free lightweight saliency map generation method. As depicted in Figure 2, Recipro-CAM extracts $K \times H \times W$ dimensional feature map F from a specified convolution layer and generates the number of $H \times W$ spatial masks. By passing the masked feature map to the rest of the architecture, the proposed method measures prediction scores of each class for feature location (u, v) imposed by each of the new input feature map's spatial masks. For simplicity, we will ignore the batch dimension in this paper.

3.1 Spatial Mask and Feature Generation

In order to highlight the importance of the each activation on feature map to the output prediction, we hide all activation except for the target pixel, which is directly mapped to the region of original input according to the receptive field as depicted in Figure 3. We suppose that the each perturbed feature map by the spatial mask can contain a relatively broad range of properties of the input image, and hence the single-position multi-channel enabled feature map can provide enough information for prediction with reduced information overlapping by other nearby positions.

By setting only one element (u, v) matched at the order of the first dimension in the feature map as 1 while 0 for others, the $H \times W$ spatial mask M^n is generated for $n = 1, \dots, N$, where N is given by HW . From the $K \times H \times W$ feature map F extracted from the specified convolution layer, the $N \times K \times H \times W$ masked feature map \tilde{F} is generated via

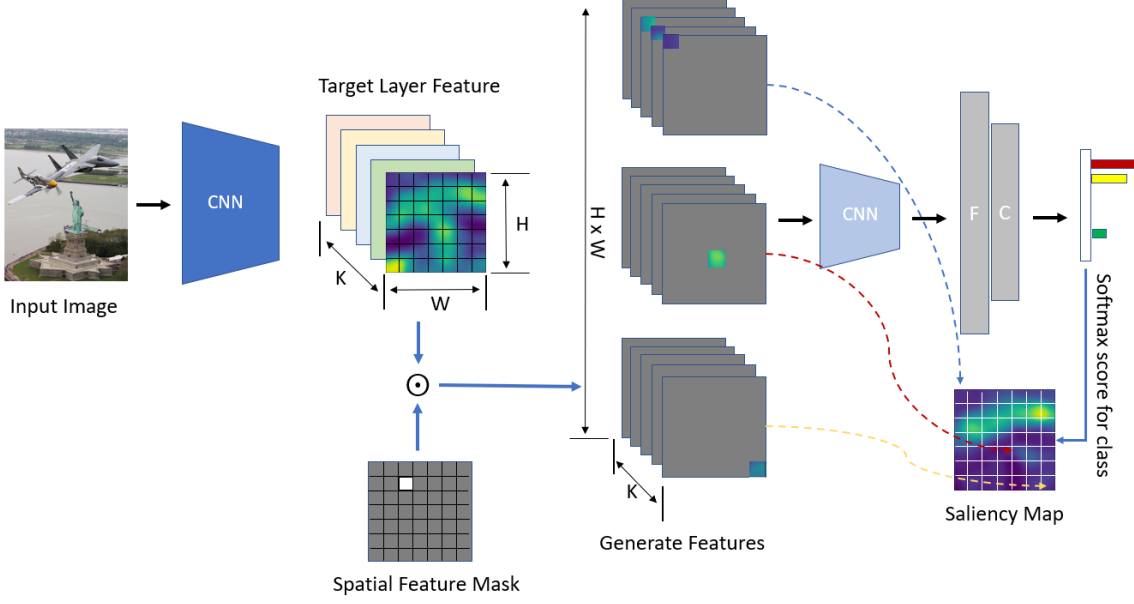


Figure 2: Overview of Recipro-CAM: Target layer’s feature map is multiplied with number of HW spatial masks which have one value at one spatial position in feature map, and the generated new HW feature maps are given as input of next part of the network, and then the predicted scores of the given class are gathered to fill saliency map’s each position. Where, K is channels, H is feature height, and W is feature width.

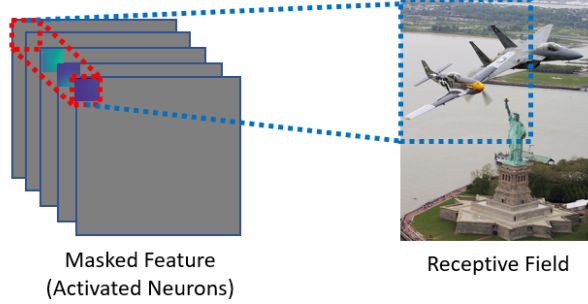


Figure 3: Sample of receptive field covered by enabled neurons marked with dashed red boxes.

element-wise multiplication with the original feature map and spatial mask M . That is, the n th masked feature map for channel k can be expressed as

$$\tilde{F}_k^n = F_k \odot M^n \quad (5)$$

with the Hardamard product \odot .

3.2 Saliency Map Generation

To generate a saliency map, Recipro-CAM separates the network into two parts according to the specified convolution layer. The first part is the feature generation network denoted as f and the second part is the next network layers denoted as g . Then a saliency map S^c for a class c can be expressed as

$$S^c = \text{reshape} \left[\frac{\mathbf{y}_c - \min(\mathbf{y}_c)}{\max(\mathbf{y}_c) - \min(\mathbf{y}_c)}, (H, W) \right], \quad (6)$$

where the $N \times 1$ prediction vector $\mathbf{y}_c = [y_c^1, \dots, y_c^N]^T$ for a class c is composed of

$$y_c^n = \text{softmax}(g(f(I) \odot M^n))_c \quad (7)$$

for $n = 1, \dots, N$.

Table 1: Evaluation of different CAM-based approaches with existing metrics, on six different backbones. Other CAM methods' evaluation scores came from [16].

Method	VGG-16						ResNet-18							
	Drop (\downarrow)	Inc (\uparrow)	Del (\downarrow)	Ins (\uparrow)	Coher (\uparrow)	Compl (\downarrow)	ADCC (\uparrow)	Drop (\downarrow)	Inc (\uparrow)	Del (\downarrow)	Ins (\uparrow)	Coher (\uparrow)	Compl (\downarrow)	ADCC (\uparrow)
Grad-CAM	66.42	5.92	11.12	19.56	69.20	15.65	53.52	42.90	16.63	13.43	41.47	81.03	23.04	69.98
Grad-CAM++	32.88	20.10	8.82	36.60	89.34	26.33	75.65	17.85	34.46	12.30	44.80	98.18	44.63	74.24
SGrad-CAM++	36.72	16.11	10.57	31.36	82.68	28.09	71.72	20.67	29.99	12.83	43.13	97.53	43.11	74.20
Score-CAM	26.13	24.75	9.52	47.00	93.83	20.27	81.66	12.81	40.41	10.76	46.01	98.35	41.78	77.30
Recipro-CAM	21.51	34.86	9.50	46.88	92.24	27.48	80.27	20.68	36.30	10.19	44.93	97.38	33.60	79.08
ResNet-50													ResNet-101	
Grad-CAM	32.99	24.27	17.49	48.48	82.80	22.24	75.27	29.38	29.35	18.66	47.47	81.97	22.51	76.40
Grad-CAM++	12.82	40.63	14.10	53.51	97.84	43.99	75.86	11.38	42.07	14.99	56.65	98.28	43.94	76.34
SGrad-CAM++	15.21	35.62	15.21	52.43	97.47	42.25	76.19	13.37	37.76	14.32	58.23	97.76	42.61	76.54
Score-CAM	8.61	46.00	13.33	54.16	98.12	42.05	78.14	7.20	47.93	14.63	59.57	98.37	42.04	78.55
Recipro-CAM	15.69	40.54	13.34	55.39	96.68	32.90	80.84	15.07	41.39	15.80	59.28	97.21	32.45	81.38
ResNeXt-50													ResNeXt-101	
Grad-CAM	28.06	29.42	20.73	50.30	82.72	25.57	76.09	24.12	36.37	20.47	61.04	82.94	25.45	77.62
Grad-CAM++	11.12	41.38	17.07	56.06	97.30	48.66	73.16	9.74	42.63	17.63	62.90	95.05	46.27	74.61
SGrad-CAM++	12.70	36.58	16.90	56.76	97.32	47.48	73.58	9.49	40.43	17.67	64.16	96.81	49.24	73.03
Score-CAM	7.20	45.70	15.59	57.92	98.00	46.86	75.38	5.37	47.70	17.30	63.61	97.03	46.83	75.60
Recipro-CAM	13.70	40.82	18.94	58.93	96.37	37.36	79.10	12.03	42.69	20.25	64.70	97.50	35.62	80.74

4 Experiments

We will show the accuracy and the effectiveness of Recipro-CAM by quantitative, qualitative, and performance analysis in Sections 4.1, 4.2, and 4.3, respectively.

4.1 Quantitative Analysis

For quantitative analysis, we use the ADCC metric suggested by Poppi et al. [2021] and follow their experimental conditions as follows. ILSVRC2012 (Russakovsky et al. [2015]) validation set (50,000) is used as an evaluation dataset and for comparing with Poppi et al. [2021] results, we also evaluate Recipro-CAM on VGG-16 (Simonyan and Zisserman [2015]), ResNet-18, ResNet-50, ResNet-101 (He et al. [2016]), ResNeXt-50, and ResNeXt-101 (Xie et al. [2017]) applying each CAM approach on the last block or convolution layer of them. The input images are resized to 256×256 and then center cropped to 224×224 . The images are normalized using mean [0.485, 0.456, 0.406] and standard deviation [0.229, 0.224, 0.225]. The Recipro-CAM's results are added to the results of Poppi et al. [2021] and the consolidated results are summarized in Table 1.

As Table 1 shows, Recipro-CAM achieves SOTA performance on ADCC metric with five architectures except for VGG-16. A closer look at the ADCC metrics shows that Score-CAM provides the highest-ranking Average Drop score for the five architectures, whereas Recipro-CAM is significantly less Complexity and this leads SOTA performance in ADCC metric combining Average Drop, Coherency and Complexity. For VGG-16, the opposite trend was observed. In terms of Coherency, Score-CAM seems generally better than the proposed method, but there is no significant difference to affect ADCC rank.

Looking at the Insertion metric, Recipro-CAM and Score-CAM take the first and second places alternately. Deletion metric usually shows similar to Insertion results, but in ResNext model, Score-CAM performance is clearly superior to the proposed method. However, it is worth-noting that the authors Poppi et al. [2021] have shown that the Average Drop, Average Increase, Insertion, and Deletion are insufficient to provide an affordable evaluation for explainability using Fake-CAM while ADCC provides a reasonable and separable assessment. This is also observed in our results as well.

4.2 Qualitative Analysis

ResNet-50 backbone architecture and Torchvision ImageNet pretrained model for the architecture is used for this evaluation, and we used torchCAM (Fernandez [2020]) library for evaluating all Grad-CAM, Grad-CAM++, Smooth Grad-CAM++, and Score-CAM saliency maps. The same pre-processing and normalization methods with Section 4.1 are used for the input images.

For systematical analysis, we categorized input images selected from the ILSVRC2012 validation dataset into three groups. The first group is for a single object-only case, the second is the same multiple objects in the input, and the third is different multiple objects in input.

The first case's results are compared in Figure 4. For the street sign, all methods focus on the bottom edge and nail head, but Score-CAM shows additional saliency on the upper pole part and Recipro-CAM shows a relatively small saliency area for treetops.

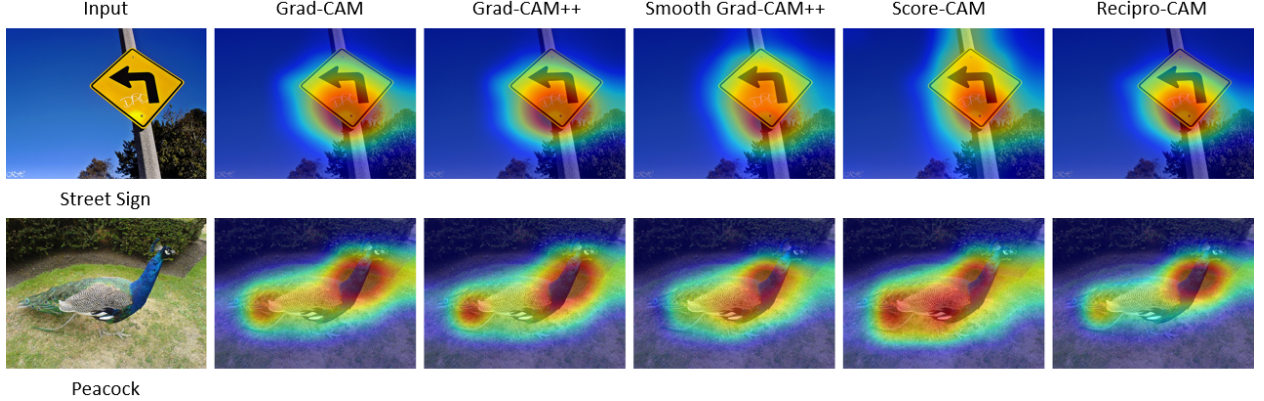


Figure 4: Single-object CAM results: Street Sign and Peacock inputs process with Grad-CAM, Grad-CAM++, Smooth Grad-CAM++, Score-CAM, and Recipro-CAM to generate saliency maps.

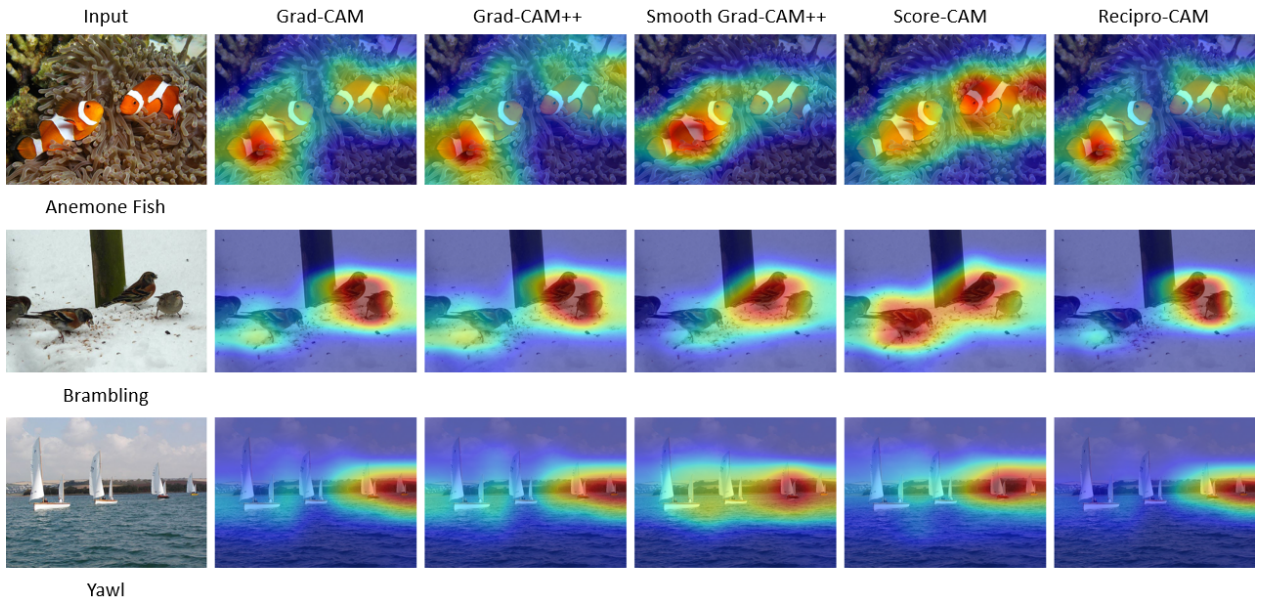


Figure 5: Same multiple-objects CAM results: Anemone Fish, Brambling, and Yawl inputs process with Grad-CAM, Grad-CAM++, Smooth Grad-CAM++, Score-CAM, and Recipro-CAM to generate saliency maps.

For the peacock case, Recipro-CAM shows an overall similar saliency pattern with Grad-CAM, and Grad-CAM++ except for the tail part, but Score-CAM's saliency map covers hole peacock and Smooth Grad-CAM++ focus on body part only. In this case, Score-CAM shows a more explainable result.

The second case is designed for evaluating the localization capability of methods and the results are compared in Figure 5. Recipro-CAM, Grad-CAM++, and Grad-CAM show the relatively separated saliency map for anemone fish, but Score-CAM shows a connected saliency map and strong activation score for coral. Smooth Grad-CAM shows a slightly connected saliency map but a low saliency score for coral. Another interesting point is that Score-CAM has a maximum saliency score at right fish, but other CAMs have maximum point at left fish.

For the brambling case, all CAMs have different saliency map patterns. Recipro-CAM and Smooth-Grad-CAM++ show relatively low saliency scores for left birds. Grad-CAM and Grad-CAM++ show similar saliency maps but Grad-CAM++ has a higher saliency score for left birds than Grad-CAM. Score-CAM gives high saliency scores for all birds so in this case, Score-CAM shows the best saliency map.

Recipro-CAM, Grad-CAM++, and Grad-CAM give similar saliency maps for the last yawl case. They show the highest saliency score at the fourth yawl from the left, but Smooth Grad-CAM++ and Score-CAM show the highest value at the third yawl from the left. In this case, Smooth Grad-CAM++ shows the best saliency map because it shows a saliency map covering all yawls.

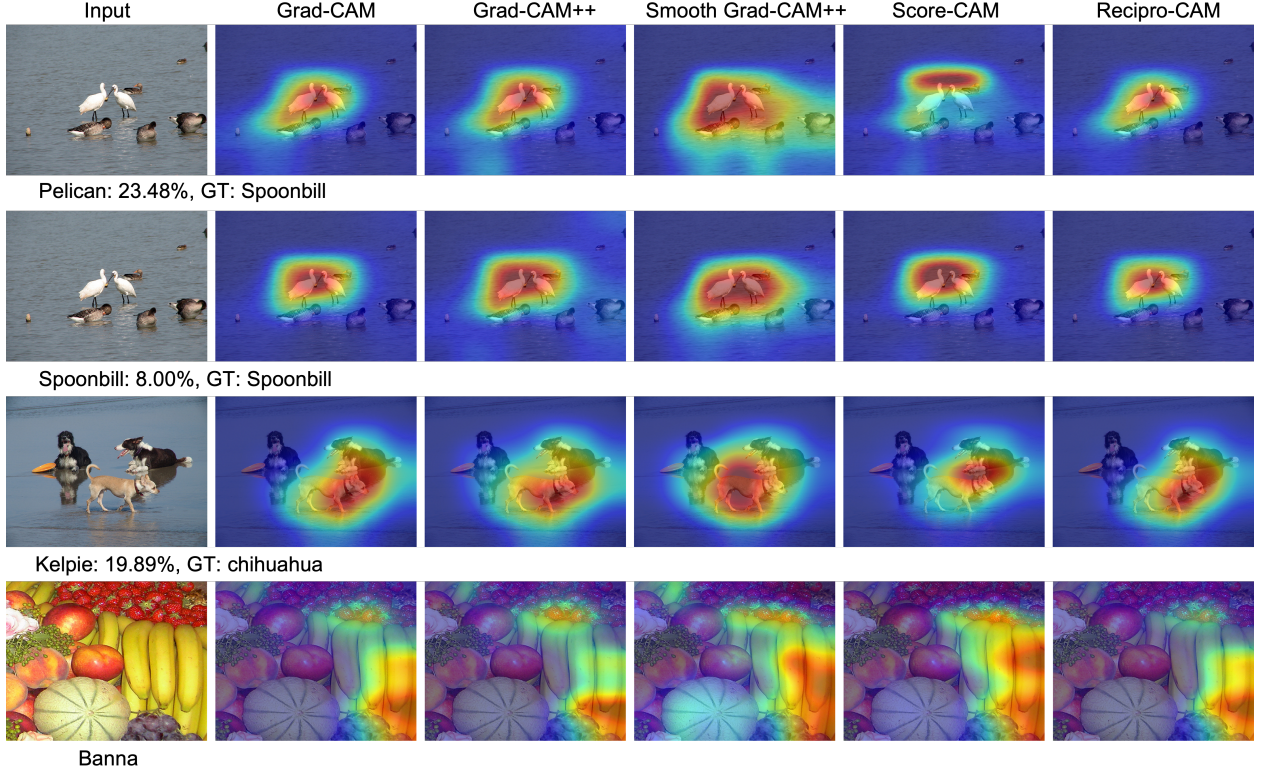


Figure 6: Multiple-objects' saliency map results: Spoonbill, Kelpie, and Banana inputs process with Grad-CAM, Grad-CAM++, Smooth Grad-CAM++, Score-CAM, and Recipro-CAM to generate saliency maps. In this analysis, Smooth Grad-CAM++ and Score-CAM showed unusual results.

The different multiple objects in the same image case are designed to check the method's resolution capability between different objects because the saliency map should show class-dependent results so different class objects should be deactivated in the image. The compared results are compared in Figure 6.

The first row of Figure 6 is the result of a spoonbill image containing mallard objects also, but ResNet-50 predicts it as pelican with a 23.48% probability. From Recipro-CAM, Grad-CAM++, and Grad-CAM results, we can assume that the root cause of the error is related to the over-focused beak part via the network, but Smooth Grad-CAM++ shows the highest saliency score at the left spoonbill body part and also the saliency map covers mallard so in this case, it couldn't separate different objects from the target class objects, and Score-CAM shows the hottest area at lake surface so in this case, it gives wrong information.

To investigate this more, we generate a spoonbill saliency map, and the results are shown in the second row all methods show similar broad coverage on body parts but Smooth Grad-CAM++ also covers mallards.

The third row also shows wrong predicted case. ResNet-50 predicts it as Kelpie with 19.89% probability, but its ground truth is chihuahua. All methods except for Smooth Gard-CAM++ show the saliency map in between second and third dogs, so it can be interpreted that ResNet-50 confused by the mixed features because Kelpie has the two dogs' features. Smooth Grad-CAM++ shows broad saliency map covering all dogs, but the hottest area is on the second dog, and this is the ground truth, so this cannot be used as good debug information.

The fourth row shows the banana's saliency map, and all CAM methods show different patterns, but they cover the banana area well except for the Smooth Grad-CAM++ method. Its' saliency map also covers pumpkins.

In overall multiple objects analysis, the Score-CAM method showed unusual results, so we need to check its resolution capability with other input and review the authors' experiment for kite image, and the results are shown in Figure 1 and Figure 7, respectively.

Figure 1 shows Recipro-CAM, Grad-CAM++, and Score-CAM's saliency maps and the ResNet-50 network predicts it as an aircraft carrier, but its ground truth is warplane. Recipro-CAM and Grad-CAM++ are highlighting the right plane and green field so we can guess that the network would be confused with the green field because the aircraft carrier has

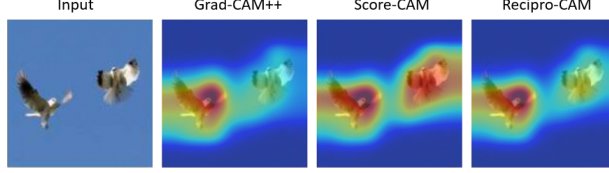


Figure 7: Kite saliency map comparison generated from Grad-CAM++, Score-CAM, and Recipro-CAM. Grad-CAM++ and Recipro-CAM highlight the kite, but Score-CAM highlights kite and pigeon. Input image is copied from (Wang et al. [2020a]).

Table 2: Execution time comparison of five methods. The execution time was measured with 1,000 inputs and calculated the average time, so the time is execution time for single image.

	Execution Time (ms)	FPS	Ratio
Recipro-CAM	13.8	72.46	-
Grad-CAM	16.0	62.50	1.16 \times
Grad-CAM++	16.2	62.73	1.17 \times
SGrad-CAM++	77.3	12.94	5.60 \times
Score-CAM	2039.7	0.49	147.80 \times

planes on its deck and in this case, the overlapped right plane and green field can give similar feature to the network. However, Score-CAM highlights two planes and even gives some saliency score for the statue of liberty so with this saliency map we cannot guess the prediction error.

Figure 7 is reproduced result of the first row of Figure 6 of (Wang et al. [2020a]) but we replace the Grad-CAM result with Recipro-CAM's. Torchvision's ResNet-50 pretrained network predicts the image as a kite with 97.46 % probability so the kite saliency map should highlight the kite only and show a lower saliency score for the other bird because the network will give a low confidence value for the other bird even though the network can be confused with similar bird's features from other bird. This is our expectation and Recipro-CAM and Grad-CAM++ give the expected results, but Score-CAM highlights the two birds all and the authors insist it as Score-CAM's superior capability.

4.3 Performance Analysis

To our knowledge, previous CAM-based (white-box approach) XAI research didn't consider their execution performance because CAM or gradient-based CAM methods are enough fast so the performance was not an issue, but Score-CAM has performance issue and its performance has dependent on the number of the feature channels, input resolution, and network capacity, so execution performance also should be one of metric for evaluating XAI method.

We conducted experiments for measuring Grad-CAM, Grad-CAM++, Smooth Grad-CAM++, Score-CAM, and Recipro-CAM's execution performance with Torchvision ResNet-50 ImageNet pretrained model. The test data is 1000 randomly selected images from the ILSVRC2012 validation dataset, and the image preprocessing and crop size is the same as the quantitative analysis process. The prepared devices are a single Nvidia Geforce RTX 3090 and a i9-11900 Intel CPU.

As described in Table 2, Recipro-CAM shows the best execution performance (Time: 13.8 ms, FPS: 72.46), and Grad-CAM and Grad-CAM++ show similar performance with Recipro-CAM, but Smooth Grad-CAM++ shows relatively low performance (Time: 77.3 ms, FPS: 12.94). The worst performance was measured from Score-CAM (Time: 2.0397 s, FPS: 0.49) and this is around 148 \times slower than Recipro-CAM, so Score-CAM has weak point in its performance.

5 Conclusion

We proposed a novel gradient-free efficient saliency map generation method Recipro-CAM and showed its superiority by quantitative and qualitative analysis. Recipro-CAM achieved state-of-the-art results on the ADCC metric and in execution time. Specifically, Recipro-CAM achieved around 148 \times faster execution performance than Score-CAM and this is faster than the gradient-based methods even though Recipro-CAM is the gradient-free method.

References

B. Zhou, A. Khosla, A. Lapedriza, A. Oliva, and A. Torralba. Learning deep features for discriminative localization. *IEEE Conference on Computer Vision and Pattern Recognition (CVPR)*, 2016.

R. R. Selvaraju, A. Das, R. Vedantam, M. Cogswell, D. Parikh, and D. Batra. Grad-cam: Why did you say that? visual explanations from deep networks via gradient-based localization. *arXiv preprint arXiv:1610.02391*, 2016.

H. Wang, Z. Wang, M. Du, F. Yang, Z. Zhang, S. Ding, P. Mardziel, and X. Hu. Score-cam: Score-weighted visual explanations for convolutional neural networks. *IEEE Conference on Computer Vision and Pattern Recognition Workshops (CVPRW)*, 2020a.

V. Petsiuk, A. Das, and K. Saenko. Rise: Randomized input sampling for explanation of black-box models. *British Machine Vision Conference (BMVC)*, 2018.

M. D. Zeiler and R. Fergus. Visualizing and understanding convolutional networks. *European Conference on Computer Vision (ECCV)*, 2014.

J. T. Springenberg, A. Dosovitskiy, T. Brox, and M. Riedmiller. Striving for simplicity: The all convolutional net. *arXiv preprint arXiv:1412.6806v3*, 2015.

A. Chattopadhyay, A. Sarkar, P. Howlader, and V. N. Balasubramanian. Grad-cam++: Generalized gradient-based visual explanations for deep convolutional networks. *IEEE Winter Conference on Applications of Computer Vision (WACV)*, 2018.

R. Fu, Q. Hu, X. Dong, Y. Guo, Y. Gao, and B. Li. Axiom-based grad-cam: Towards accurate visualization and explanation of cnns. *British Machine Vision Conference (BMVC)*, 2020.

D. Omeiza, S. Speakman, C. Cintas, and K. Weldermariam. Smooth grad-cam++: An enhanced inference level visualization technique for deep convolutional neural network models. *arXiv preprint arXiv:1908.01224*, 2019.

J. Bai, F. Lu, K. Zhang, et al. ONNX: Open neural network exchange, 2019. URL <https://github.com/onnx/onnx>.

Intel. OpenVINO toolkit, 2019. URL <https://software.intel.com/enus/openvino-toolkit>.

H. Wang, R. Naidu, J. Michael, and S. S. Kundu. Ss-cam: Smoothed scorecam for sharper visual feature localization. *arXiv preprint arXiv:2006.14255*, 2020b.

R. Naidu, A. Ghosh, Y. Maurya, and S. S. Kundu. Is-cam: Integrated scorecam for axiomatic-based explanations. *arXiv preprint arXiv:2010.03023*, 2020.

S. Desai and H. G. Ramaswamy. Ablation-cam: Visual explanations for deep convolutional network via gradient-free localization. *IEEE Winter Conference on Applications of Computer Vision (WACV)*, 2020.

A. S. Morcos, D. G. Barrett, N. C. Rabinowitz, and M. Botvinick. On the importance of single directions for generalization. *IEEE Conference on Learning Representations (ICLR)*, 2018.

E. M. Kenny, C. Ford, M. Quinn, and M. T. Keane. Explaining black-box classifiers using post-hoc explanations-by-example: The effect of explanations and error-rates in xai user studies. *Artificial Intelligence*, 2021.

P. Dabkowski and Y. Gal. Real time image saliency for black box classifiers. *Neural Information Processing Systems (NeurIPS)*, 2017.

V. Petsiuk, R. Jain, V. Manjunatha, V. I. Morariu, A. Mehra, V. Ordonez, and K. Saenko. Black-box explanation of object detectors via saliency maps. *IEEE Conference on Computer Vision and Pattern Recognition (CVPR)*, 2020.

S. Poppi, M. Cornia, L. Baraldi, and R. Cucchiara. Revisiting the evaluation of class activation mapping for explainability: A novel metric and experimental analysis. *IEEE Conference on Computer Vision and Pattern Recognition (CVPR)*, 2021.

O. Russakovsky, J. Deng, H. Su, J. Krause, S. Satheesh, S. Ma, Z. Huang, A. Karpathy, A. Khosla, M. Bernstein, A. C. Berg, and L. Fei-Fei. Imagenet large scale visual recognition challenge. *International Journal of Computer Vision*, (3):211–252, 2015.

K. Simonyan and A. Zisserman. Very deep convolutional networks for large-scale image recognition. *International Conference on Learning Representations (ICLR)*, 2015.

K. He, X. Zhang, S. Ren, and J. Sun. Deep residual learning for image recognition. *IEEE/CVF Conference on Computer Vision and Pattern Recognition (CVPR)*, 2016.

S. Xie, R. Girshick, P. Dollar, Z. Tu, and K. He. Aggregated residual transformations for deep neural networks. *IEEE/CVF Conference on Computer Vision and Pattern Recognition (CVPR)*, 2017.

F.-G. Fernandez. Torchcam: class activation explorer. 2020. URL <https://github.com/frgfm/torch-cam>.